Journal of the Korean Nuclear Society
Volume 34, Number 6, pp.533 ~ 544, December, 2002

Neutron Cross Section Evaluation on Mo-95, Tc-99, Ru-101 and Rh-103 in the Fast Energy Region

Y. D. Lee and J. H. Chang
Korea Atomic Energy Research Institute
150 Dukjin-dong, Yuseung-gu, Daejeon 305-353, Korea
ydlee@kaeri.re.kr

(Received May 15, 2002)

Abstract

The neutron induced nuclear data for Mo-95, Tc-99, Ru-101 and Rh-103 was calculated and evaluated in the fast energy region. The energy dependent optical model potential parameters were extracted based on the recent experimental data and applied up to 20 MeV. The s-wave strength function was calculated from the parameters. Spherical optical model, statistical model in equilibrium energy, multistep direct and multistep compound model in pre-equilibrium energy and direct capture model were used in the calculation. The theoretically calculated cross sections were compared with the experimental data and the evaluated files. The model-calculated total and capture cross sections were in good agreement with the reference experimental data. The direct capture contribution improved the capture cross sections in pre-equilibrium region. The evaluated cross section results were compiled to ENDF-6 format and will improve the ENDF/B-VI.

Key Words : evaluation, neutron cross section, fission product

1. Introduction

The neutron cross section evaluation for the selected fission products[1] which mainly influence a reactivity in a fission reactor has been jointly done with National Nuclear Data Center (NNDC) of Brookhaven National Laboratory (BNL). The current work was the continuity to the resonance evaluation[2]. The joint work is divided into two regions: resonance region including thermal region and upper resonance region up to 20 MeV. Different theories and procedures were applied in each energy region for cross section calculation and evaluation. For resonance energy region, the evaluation was done for all the selected fission products[3] and the results were adopted in ENDF/B-VI last year up to unresolved energy region. Unresolved resonance region is extended up to several tens of keV or hundreds of keV for the selected fission products. The current evaluation results will complement the evaluation of the resonance region. In this paper, the evaluated results of Mo-95, Tc-99, Ru-101 and Rh-103 are presented from 10 keV up to 20

MeV. Later, the other fission product nuclei will be evaluated.

Neutron-induced nuclear reaction data for fission products are important for burnup performance prediction in a fission reactor, criticality calculation for spent fuel storage design, advanced fuel performance analysis and radiation damage estimation of structural material. Neutron capture cross sections in several keV region are important in several applications concerning neutron absorption.

Mo-95, Ru-101 and Rh-103 are stable isotopes and Tc-99 has very long life time. They are mainly accumulated from beta decay and electron capture in a fission reactor. Mo-95 is sometimes used as additive material in alloy and Tc-99 used as super-conducting material. Therefore, improved neutron cross section data are required. In ENDF/B-VI, the revision was made in 1999 for these isotopes up to the 1st excited energy level using recently evaluated resonance parameters[3]. However, for higher energy region, the modifications on Mo-95 and Ru-101 were done in 1980 and 1991, respectively, and Tc-99 and Rh-103 in 1978. In ENDF/B-VI, the Moldauer potential parameters[4] for Mo-95 and Ru-101 were used to produce the total cross section and the Auerbach potential for Tc-99 and Rh-103. These potential parameters were obtained in 1963 and 1964. In ENDF/B-VI, for Ru-101, only capture cross section was revised based on the Macklin data[4]. The capture cross section for Tc-99 and Rh-103 was produced by the least square fitting process. Therefore, in the current evaluation for higher energy region, the energy-dependent optical model potential parameters were newly searched and the quantum mechanical models were applied based on the recent experimental data.

The evaluation consists of optical model potential search followed by complete nuclear reaction model calculation and validation to the experimental data. The potential parameters were decided by comparing the model calculated total and elastic scattering cross sections with the reference experimental data. The s-wave strength function calculated by the extracted potential parameters was compared with that by the resonance parameters in the resonance region.

Nuclear reaction cross sections were calculated by using the recently released Empire-II code[5]. Direct capture model was recently inserted into Empire to enhance capture cross section in pre-equilibrium region. Empire also offers several built-in libraries including the ENSDF nuclear level and decay schemes, nuclear masses, ground state deformations and γ-ray strength functions. The discrete energy levels were searched to match with the continuum. The calculated cross sections were graphically compared with the experimental data and the evaluated files (ENDF/B-VI, JENDL-3.2, JEF-2.2, BROND-2 and CENDL-2). The evaluated results were compiled to ENDF-6 format.

2. Theory

2.1. Optical Model Potential

RIPL neutron potential library[6] was examined to compare the total cross section and the s-wave strength function produced in optical model with the reference data. The comparison was not satisfactory. Therefore, new potential parameters were required for better cross section production. To obtain proper potential parameters, the Woods-Saxon well[7] is used for the real part potential:

$$V(r) = -V/[1+\exp((r-R_v)/a_v)] \quad (1)$$

where V and a_v are the strength and diffuseness of the potential. The nuclear radius R_v, related to mass number A, is given by

$$R_v = r_v A^{1/3}. \quad (2)$$

For the imaginary part potential, the derivative Woods-Saxon shape is used,

$$W(r) = -4W\exp((r-R_w)/a_w) /[1+ \exp((r-R_w)/a_w)]^2 \quad (3)$$

where W, R_w and a_w are potential strength, radius and diffuseness, respectively. Generally, Thomas form is taken in the optical model potential for spin-orbit coupling:

$$V_{s\text{-}o}(r)=(2\boldsymbol{L}\cdot\boldsymbol{S})V_{so}(2/r)d\{1/[1+\exp((r-R_{so})/a_{so})]\}/dr \quad (4)$$

where $\boldsymbol{L}\cdot\boldsymbol{S}$ is the dot product of the orbital and spin angular momentum operators.

The optical model potential form was constructed as a function of the incident neutron energy and the corresponding parameters were searched interactively in a spherical optical model based on the reference experimental data. The real and imaginary potential strength and radius parameters were expanded:

$$V = V_0 + V_1 E_n, \quad r_v = r_0 + r_1 E_n \quad (5a)$$

$$W = W_0 + W_1 E_n, \quad r_w = r_{wo} + r_{w1} E_n \quad (5b)$$

where E_n is an incident neutron energy. The potential parameters (V_o, V_1, W_o, W_1, r_o, r_1, r_{wo}, r_{w1}, a_v, a_w, V_{so}, r_{so}, a_{so}) were searched simultaneously. As an initial value, JENDL parameters[8] were used. The parameter searching process was described in the previous work[2]. The decided potential was used to produce transmission coefficients, s-wave strength function value, total, shape elastic and reaction cross sections for further Empire run.

2.2. Reaction Cross Section

Empire-II is a nuclear reaction code, comprising various nuclear models, and designed for calculations in a broad range of energies and incident particles. The code accounts for the major nuclear reaction mechanisms, such as optical model, Multistep Direct (MSD), Multistep Compound (MSC) and the full featured Hauser-Feshbach model. The statistical model used in the Empire-II is an advanced implementation of the Hauser-Feshbach theory with width fluctuation correction for decay of particles and gamma rays.

In the statistical model of nuclear reactions, the Compound Nucleus (CN) state a with spin J, parity Π and excitation energy E to a channel b is given by the ratio of the channel width Γ_b to the total width $\Gamma_b = \Sigma_c\Gamma_c$ multiplied by the population of this state $\sigma_a(E,J,\Pi)$. This also holds for secondary Compound Nuclei which are formed due to subsequent emissions of particles. Each of such states contributes to the cross section.

$$\sigma_b(E,J,\Pi) = \sigma_a(E,J,\Pi)\frac{\Gamma_b(E,J,\Pi)}{\sum_c \Gamma_c(E,J,\Pi)} \quad (6)$$

These have to be summed over spin J and parity Π and integrated over excitation energy E (in case of daughter CN) to obtain observable cross sections.

The particle decay width[5] is given by

$$\Gamma_c(E,J,\Pi) = \frac{1}{2\pi\rho_{CN}(E,J,\Pi)}\sum_{J'=0}^{\infty}\sum_{\Pi'}\sum_{j=J'-J}^{J+J'}\int_0^{E-B_c}\rho_c(E',J',\Pi')T_c^{l,j}(E-B_c-E')dE', \quad (7)$$

where B_c is the binding energy of particle c in the compound nucleus, ρ_c is the level density, and $T_c^{l,j}(\varepsilon)$ stands for the transmission coefficient for particle c having channel energy $\varepsilon = E - B_c - E'$ and orbital angular momentum l, which together with the particle spin s couples to the channel angular momentum j. For the discrete levels,

characterized by the energy E_i, spin J_i and parity Π_i, the level density $\rho_c(E,J',\Pi')$ reduces to $\delta(E - E_i)d_{J',J_i}\delta_{\Pi',\Pi_i}$.

The emission of neutrons, protons, α-particles, and light ions is taken into account along with the competing fission channel. Particular attention is dedicated to the determination of the level densities, which can be calculated in the non-adiabatical approach allowing for the rotational and vibrational enhancements. Level densities acquire dynamic features through the dependence of the rotational enhancement in the shape of a nucleus.

The dynamic approach[5] to the level densities is specific to the Empire-II code. It takes into account collective enhancements of the level densities due to nuclear vibration and rotation. The level density is corrected for rotational and vibrational collective effects in the non-adiabatic mode. In the case of the oblate nuclei which are assumed to rotate parallel to the symmetry axis, the level density is expressed as[5]

$$\rho(E,J,\Pi) = \frac{1}{16\sqrt{6\pi}}\left(\frac{\hbar^2}{\Im_{\parallel}}\right)^{1/2} a^{1/4} \sum_{K=-J}^{J} \left(U - \frac{\hbar^2[J(J+1)-K^2]}{2|\Im_{eff}|}\right)^{-5/4} \exp\left\{2\left[a\left(U - \frac{\hbar^2[J(J+1)-K^2]}{2|\Im_{eff}|}\right)\right]^{1/2}\right\}. \quad (8)$$

Here, a is a level density parameter, J is a nucleus spin and K is its projection. E is the excitation energy, U is the excitation energy less pairing (Δ), $\Im_{eff}$ is the effective moment of inertia and $\Im_{\parallel}$ is the parallel component.

Gilbert-Cameron[9] approach does not account explicitly for the collective enhancements of the level densities. The dynamical approach[5] to the level densities was used in Empire calculation. Level density parameter, a, was assumed to be energy dependent of incident neutron and calculated following Ignatyuk et al[10] as

$$a(U) = \tilde{a}\left[1 + f(U)\frac{\delta_W}{U}\right]. \quad (9)$$

δ_W is the shell correction which fade-out with increasing energy and $\tilde{a}$ is the asymptotic value of the a parameter. In Empire, $f(U)$ is used as a function of U.

$$f(U) = 1 - \exp(-\gamma U) \quad (10)$$

where γ = - 0.054 from Ignatyuk.

3. Evaluation

3.1. Evaluation Procedure

As a preliminary step, we retrieve and analyze the available experimental data and the evaluated files (ENDF/B-VI, JENDL-3, JEF-2, BROND-2 and CENDL-2) in the evaluation energy range. The optical model potential mainly based on the reference total and elastic scattering experimental data is searched and the potential is applied for total, elastic scattering and reaction cross sections data calculation as well as transmission coefficients for compound reaction calculation. Using these data, Empire calculates the individual reaction cross sections with level density. The calculated cross sections are formatted in ENDF-6 and compared graphically with experimental data and evaluated files. A tuning process is necessary to fit the calculated results to the reference experimental data in Empire input. If the individual cross section results are satisfied in an evaluation energy range, the results are combined with the resonance results. The created full set of nuclear data experiences format and physics checking using CHECKR, FIZCON and PSYCHE.

3.2. Results

Some important total and capture cross section experimental data are summarized in Table 1 for each nucleus. Unfortunately, there is no total cross section experimental data on Ru-101. Based on

Table 1. Reference Experimental Data and 1st Excited Energy

Isotope	Reference experimental data	
	Total cross section	(n, γ) cross section
Mo-95	Pasechnik[11]	Musgrove[12]
Tc-99	Foster[13]	Macklin[14]
Ru-101	-	Hockenbury[12]
Rh-103	Bokhovko[17]	Bokhovko[17]

Table 2. Potential Parameters as a Function of Incident Neutron Energy

Parameter(unit)	Mo-95	Tc-99	Ru-101	Rh-103
V_o(MeV)	46.00	47.50	47.50	46.81
V_1(MeV)	-0.25	-0.30	0.00	-0.40
r_o(fm)	1.291	1.290	1.282	1.234
a_v(fm)	0.670	0.620	0.620	0.665
W_o(MeV)	7.000	9.740	9.740	7.906
r_{wo}(fm)	1.401	1.425	1.415	1.450
a_w(fm)	0.410	0.350	0.410	0.437
V_{so}(MeV)	7.000	7.000	7.000	7.033
r_{so}(fm)	1.291	1.290	1.282	1.241
a_{so}(fm)	0.620	0.620	0.620	0.500
W_1(MeV)	0.0000	0.1000	0.0000	-0.1138
r_{w1}(fm)	0.000	0.000	0.000	0.000
r_1(fm)	0.000	0.000	0.000	-0.010

Table 3. Comparison of s-wave Strength Function

Isotopes	s-wave strength function	
	In ABAREX	Reference[3]
Mo-95	0.51E-4	0.45E-4
Tc-99	0.43E-4	0.43E-4
Ru-101	0.62E-4	0.62E-4
Rh-103	0.53E-4	0.57E-4

the experimental data in Table 1, the searched potential parameters are summarized in Table 2. The potential depths for the real and imaginary potentials have the range from 46.0 MeV to 47.5 MeV and from 7.0 MeV to 9.7 MeV. The radius varies from 1.23 fm to 1.29 fm for the real and from 1.40 fm to 1.45 fm for the imaginary part. The parameters are not changed significantly for the different isotopes.

The s-wave strength function (S_o) was calculated

Table 4. Discrete Energy Levels Used for Reaction Cross Section Calculation

Reaction / Isotope	Residual discrete energy levels (MeV)					
	compound	(n, n′)	(n, p)	(n, a)	(n, 2n)	(n, 3n)
Mo-95	0.0	0.0	0.0	0.0	0.0	0.0
	0.778	0.204	0.236	0.934	0.871	0.943
	1.148	0.766		1.383	1.574	1.363
	1.330	0.786		1.495	1.742	
	1.498	0.821		1.847	1.864	
	1.626			2.067		
	1.628					
	1.870					
Tc-99	0.0	0.0	0.0	0.0	0.0	0.0
	0.172	0.141	0.098	0.044	0.022	0.097
	0.201	0.143	0.236			0.216
		0.181	0.351			0.324
		0.509	0.525			
		0.534				
		0.537				
		0.612				
		0.625				
		0.653				
Ru-101	0.0	0.0	0.0	0.0	0.0	0.0
	0.475	0.127	0.009	0.735	0.540	0.09
	0.944	0.307	0.016	0.787	1.130	0.322
	1.103	0.311	0.208	1.432	1.227	0.341
	1.106	0.325	0.288	1.510	1.362	0.443
		0.344		1.758		0.576
		0.422				0.618
		0.527				0.720
						0.734
						0.897
Rh-103	0.0	0.0	0.0	0.0	0.0	0.0
	0.051	0.04	0.003	0.172	0.042	0.157
	0.097	0.093			0.105	0.182
		0.295				0.306
		0.357				0.355
		0.537				0.478
		0.607				
		0.650				
		0.652				
		0.658				
		0.780				

at 1 keV in the optical model by the searched potential parameters. As shown in Table 3, the calculated So values are close to those obtained by the recently evaluated resonance parameters[3] in unresolved resonance region. Therefore, the S_0 will help to connect smoothly the results of the two different evaluation energy regions of the different models in the unresolved region. Especially, for Ru-101, the referenced So value played an important role in total cross section calculation.

By the dynamic approach for level density, specified in the Empire, the discrete excited energy levels for the residual nuclei were limited in each reaction. These discrete levels were matched with the continuum levels. This discrete level search is needed in reaction cross section calculation. Table 4 shows the residual discrete energy levels for each reaction.

The upper energy of the unresolved resonance region was set to the energy where the inelastic scattering reaction channel opens, which is 204 keV, 141 keV, 127 keV and 40 keV for Mo-95, Tc-99, Ru-101 and Rh-103 respectively. The cross sections were evaluated on (n, tot), (n, n), (n, n′), (n, 2n), (n, 3n), (n, nα), (n, np), (n, γ), (n, p) and (n, α) from 10 keV to 20 MeV. However, in this paper, only the results on (n, tot), (n, n), (n, n′), (n, γ) and (n, p) are represented. Fig. 1 shows the comparison of the calculated result to the experimental data[11] and ENDF/B-VI for total cross section of Mo-95. The total cross section calculated by the searched optical model potential was in good agreement with the experimental

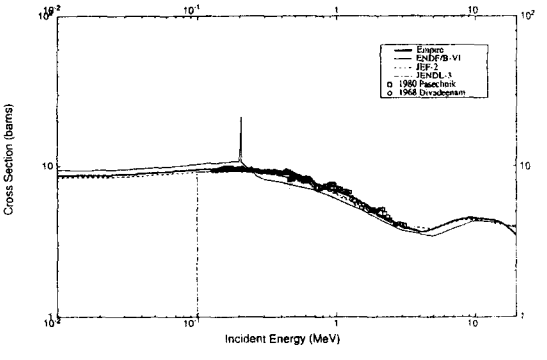

Fig. 1. Total Cross Section of Mo-95

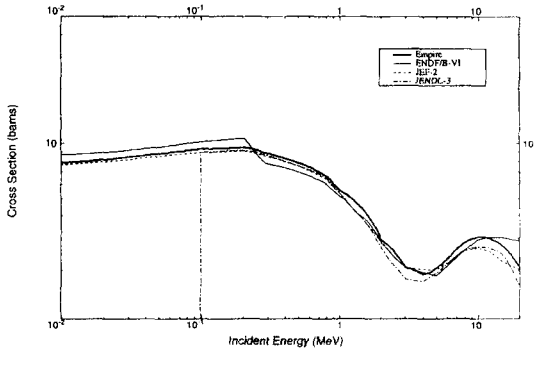

Fig. 2. (n, n) Cross Section of Mo-95

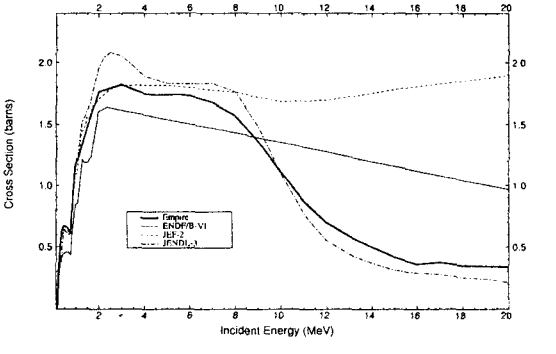

Fig. 3. (n, n′) Cross Section of Mo-95

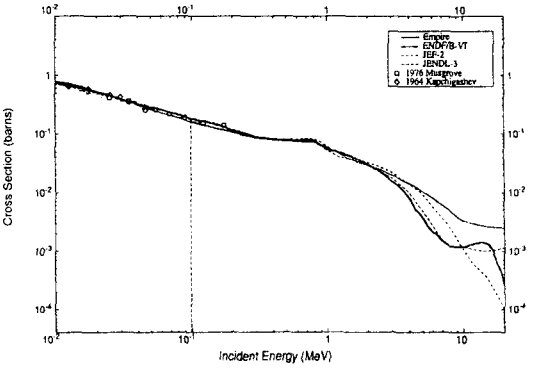

Fig. 4. (n, γ) Cross Section of Mo-95

data. ENDF/B-VI shows the difference from the calculation and the experimental data in the whole energy region. Fig. 2 shows the (n, n) cross section. There is no experimental data in this reaction. The calculation does not agree well with ENDF/B-VI. Fig. 3 is the (n, n′) cross section. ENDF/B-VI linearly decreases after 1 MeV and is higher than the calculation above 9 MeV. Fig. 4 shows the (n, γ) cross section results. The calculation follows the experimental data[12] very well and shows the direct capture contribution in the pre-equilibrium region by de-excitation of GDR around 14 MeV. There is good agreement for capture cross section between the ENDF/B-VI and the calculation up to 3 MeV. Fig. 5 is for the (n, p) cross section. The calculated result is in good agreement with the experimental data. No ENDF/B-VI data was found for this reaction.

Fig. 6 shows the calculated total cross section with the experimental data[13] and the evaluated files for Tc-99. The model calculation follows the reference experimental data well. There is a difference between the calculation and ENDF/B-VI in lower energy region. At low energies, the s-wave strength function value was referenced from the evaluation of resonance parameters. Fig. 7 shows the (n, n) cross section. There is no experimental data. The current calculation shows much difference from ENDF/B-VI. Fig. 8 shows the (n, n′) cross section. There is one experimental data at 14.7 MeV. Fig. 9 shows the capture cross section. Above 2 MeV, there is some difference between the calculation and the ENDF/B-VI. However, in the measurement energy range, both are in good agreement with the experimental data[14]. Fig. 10 is for (n, p)

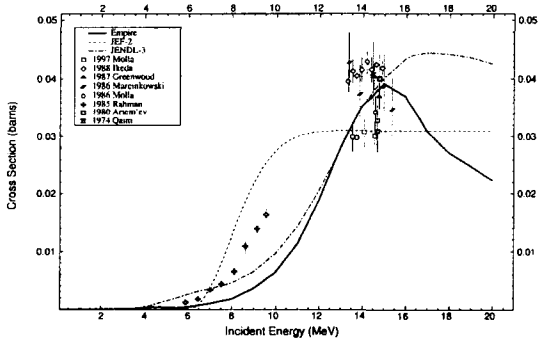

Fig. 5. (n, p) Cross Section of Mo-95

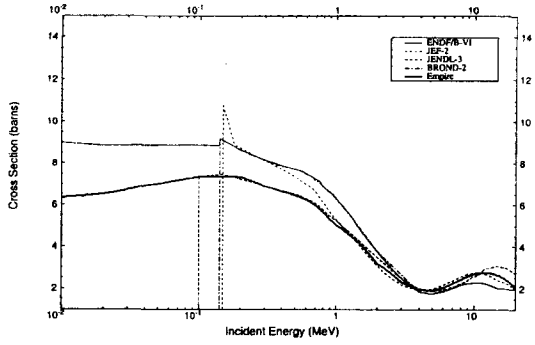

Fig. 7. (n, n) Cross Section of Tc-99

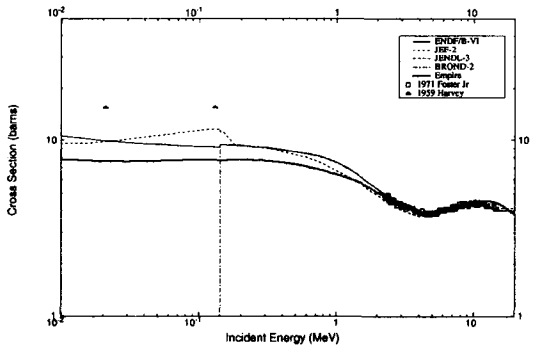

Fig. 6. Total Cross Section of Tc-99

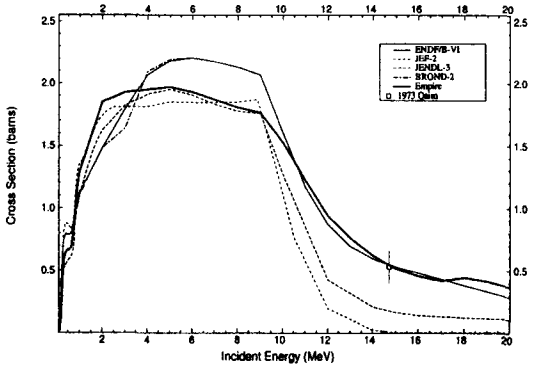

Fig. 8. (n, n′) Cross Section of Tc-99

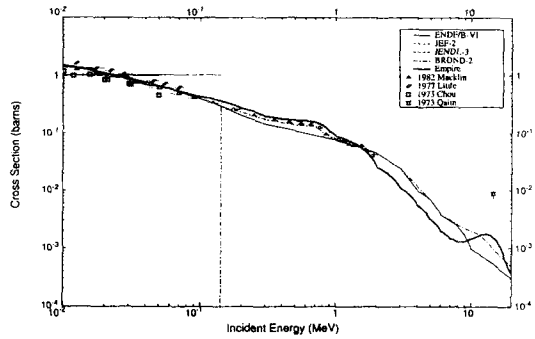

Fig. 9. (n, γ) Cross Section of Tc-99

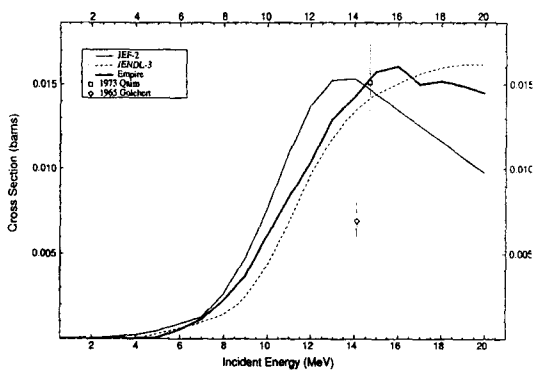

Fig. 10. (n, p) Cross Section of Tc-99

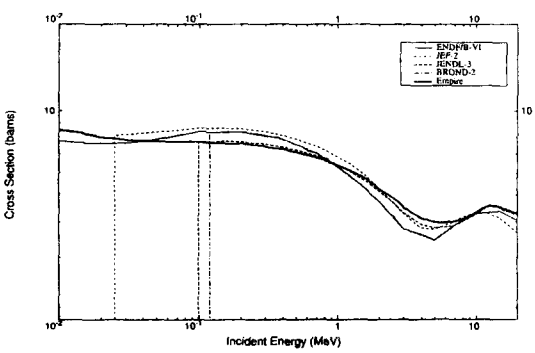

Fig. 11. Total Cross Section of Ru-101

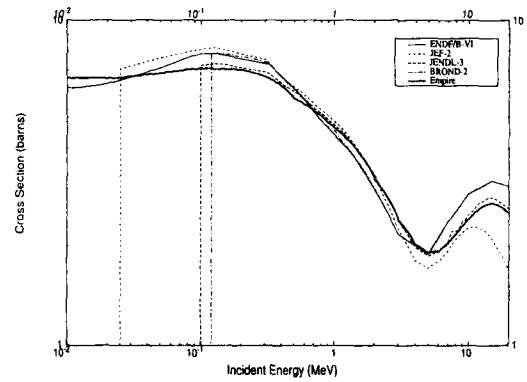

Fig. 12. (n, n) Cross Section of Ru-101

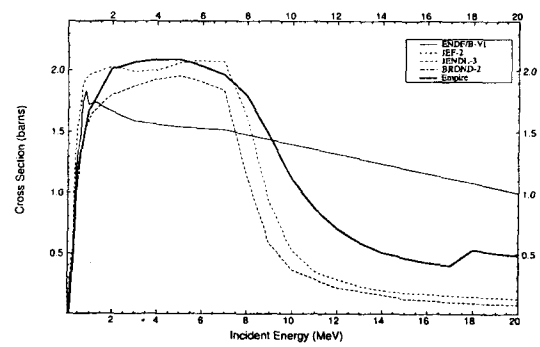

Fig. 13. (n, n′) Cross Section of Ru-101

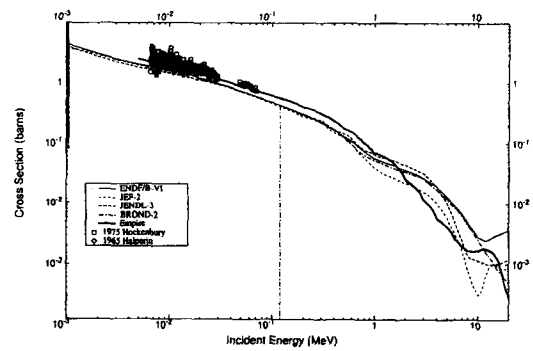

Fig. 14. (n, γ) Cross Section of Ru-101

cross section. The calculation is in good agreement with Qaim[15] data at 14.7 MeV.

The total cross section for Ru-101 was calculated and compared with the evaluated files in Fig. 11. There is no experimental data. Therefore, at low energies, the s-wave strength function value from the evaluation of resonance parameters[3] was referenced to generate the total cross section value. Fig. 12 and 13 are the (n, n) and (n, n′) cross sections. Fig. 14 shows the capture cross

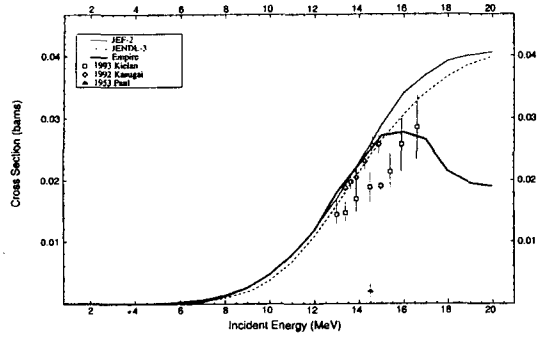

Fig. 15. (n, p) Cross Section of Ru-101

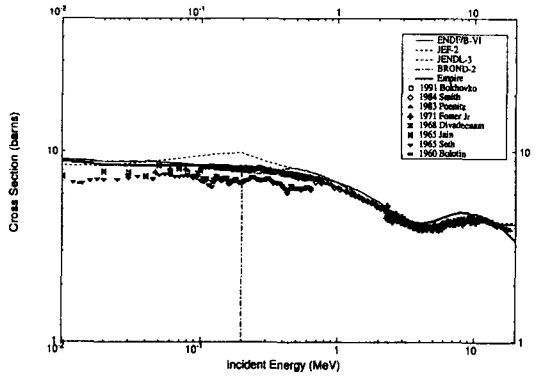

Fig. 16. Total Cross Section of Rh-103

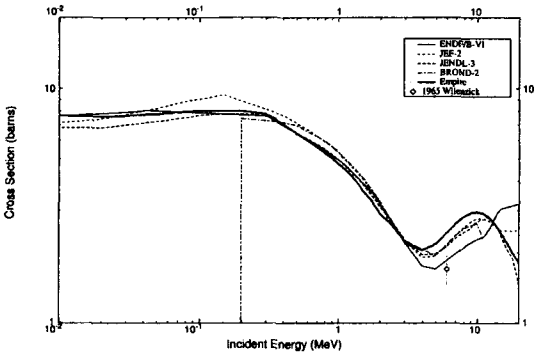

Fig. 17. (n, n) Cross Section of Rh-103

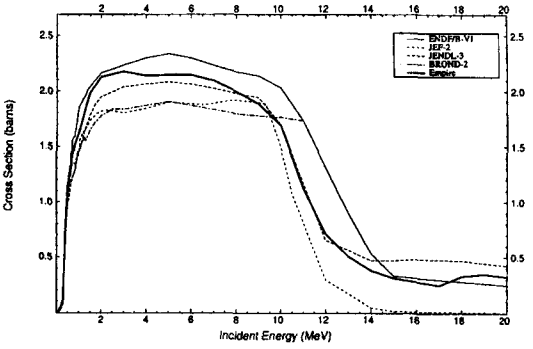

Fig. 18. (n, n′) Cross Section of Rh-103

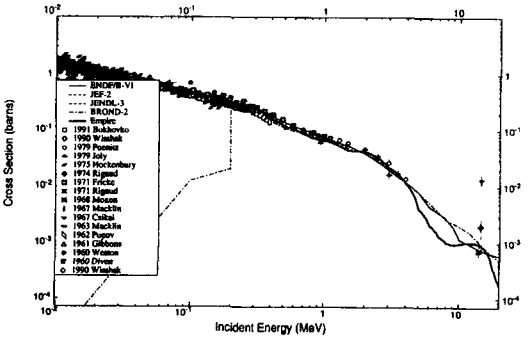

Fig. 19. (n, γ) Cross Section of Rh-103

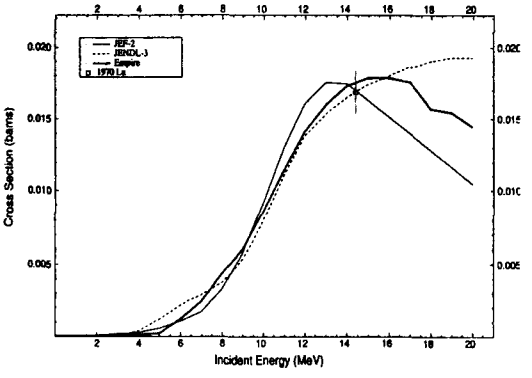

Fig. 20. (n, p) Cross Section of Rh-103

section. The calculated capture cross section is in good agreement with the reference experimental data[16]. ENDF/B-VI is lower than the calculation and experimental data in the measured energy range. Fig. 15 shows (n, p) cross section. There is an agreement with the experimental data.

Fig. 16 shows the total cross section of Rh-103. The calculation is in good agreement with the measured data[17]. The calculation is pretty close to ENDF/B-VI in the whole region. Fig. 17 is for (n, n) cross section. Fig. 18 shows (n, n′) cross section. Fig. 19 is the capture cross section. Model

calculation shows good agreement with the measured data [17] and ENDF/B-VI. Fig. 20 is for (n, p) cross section. The other threshold reaction cross sections are not shown here, but the results were summarized in ENDF-6 formatted files. The current evaluation results will be merged with the evaluation for resonance part at the 1st excited energy to make a full set of nuclear data.

4. Conclusions

The searched energy dependent optical model potential was proper to produce the calculated cross sections in the evaluation energy range. The s-wave strength function was helpful in obtaining the total cross section closer to the experimental data. Especially, when there is no experimental data for total cross section like Ru-101, the reference s-wave strength function value played a crucial role. Empire was successful in producing the reaction cross sections. Evaluated cross sections were in good agreement with the experimental data. However, some evaluated reaction cross sections showed the difference from the ENDF/B-VI. The results represented improvement over the ENDF/B-VI. All evaluated results were converted into the ENDF-6 format and will be submitted to ENDF/B-VI for a new version.

Acknowledgements

This work is performed under the auspices of Korea Ministry of Science and Technology as a long-term R&D project.

References

1. J.H. Chang et al., Establishment of Nucelar Data System, KAERI/RR-2121/(2000).
2. Y.D. Lee and J.H. Chang, "Neutron Cross Section Evaluation on Pr-141, Nd-143, Nd-145, Sm-147 and Sm-149," J. of KNS to be published, (2002).
3. S.Y.Oh and J.H.Chang, Neutron Cross Section Evaluations of Fission Products below the Fast Energy Region, BNL-NCS-67469 (KAERI/TR-1511/2000), Brookhaven Natoinal Laboratory.
4. P.F. Rose, Ed., "ENDF/B-VI Summary Documentation," BNL-NCS-17541 (ENDF-201), National Nuclear Data Center, BNL, (1991).
5. M.Herman, Empire-II: Statistical Model Code for Nuclear Reaction Calculations, IAEA, (2000).
6. S. Igarasi, Optical Model Potentials used in JENDL Evaluations (JAERI, Tokaimura, Japan), Reference Input Parameter Library for theoretical calculations of nuclear reactions (RIPL), JAERI 1228(41), (1973).
7. R.D.Lawson, ABAREX_A Neutron Spherical Optical-Statistical Model Code, in Workshop on Computation and Analysis of Nuclear Data Relevant to Nuclear Energy and Safety, pp447, Trieste, Italy.
8. T. Nakagawa, et al., Japanese Evaluated Nuclear Data Library, Version 3, Revision 2, J. Nucl. Sci. Technol. 32, 1259, (1995).
9. A. Gilbert and A.G.W. Cameron, Can. J. Phys. 43, 1446, (1965).
10. A.V. Ignatyuk, G.N. Smirenkin and A. S. Tishin, Sov. J. Nucl. Phys. 21, 255, (1975).
11. M.V. Pasechnik et al., "Total Neutron Cross Sections for Molybdenum and Zyrconium at Low Energies," C, 80KIEV, 1, 304, (1980).
12. A.R.DEL.Musgrove et al., "Average Neutron Resonance Parameters and Radiative Capture Cross Sections for the Isotopes of Molybdenum," J, NP/A, 270, 108, (1976).
13. D.G.Foster JR, D.W. Glasgon, "Neutron Total Cross Sections, 2.5 - 15 MeV," J, PR/C, 3, 576, (1971).

14. R.L. Macklin, "Technetium-99 Neutron Capture Cross Section," J, NSE, 81, 520, (1982).
15. S.M. Qaim, "Nuclear Reaction Cross-Sections for 14.7 MeV Neutrons on TC-99," J, JIN, 35, 3669, (1973).
16. R. W. Hockenbury, "Capture Cross sections of 145-Nd, 149-Sm, 101-Ru, 102-Ru, and 104-Ru," Bull. Amer. Phys. Soc., Vol.20, pp560, (1975).
17. M.V. Bokhovko et al., "Neutron Radiation Cross-Section, Neutron Transmission And Average Resonance Parameters For Some Fission Product Nuclei," R, FEI-2168-91, (1991).